Cononsolvency-Induced Micellization of Pyrene End-Labeled Diblock Copolymers of *N*-Isopropylacrylamide and Oligo(ethylene glycol) Methyl Ether Methacrylate

Jingyi Rao, Jian Xu, Shizhong Luo, and Shiyong Liu*

Department of Polymer Science and Engineering, Joint Laboratory of Polymer Thin Films and Solution, Hefei National Laboratory for Physical Sciences at the Microscale, University of Science and Technology of China, Hefei, Anhui 230026, China

Received July 6, 2007. In Final Form: August 26, 2007

Pyrene end-labeled double hydrophilic diblock copolymers, poly(*N*-isopropylacrylamide)-*b*-poly(oligo(ethylene glycol) methyl ether methacrylate) (*Py*-PNIPAM-*b*-POEGMA), were synthesized via consecutive reversible addition-fragmentation chain transfer polymerization using a pyrene-containing dithioester as the chain transfer agent. These diblock copolymers molecularly dissolve in pure methanol and water, but form well-defined and nearly monodisperse PNIPAM-core micelles in an appropriate mixture of them due to the cononsolvency of PNIPAM block. ^{1}H NMR, laser light scattering, fluorescence spectroscopy, and transmission electron microscopy were employed to characterize the cononsolvency-induced PNIPAM-core micelles. When the volume fraction of water, φ_{water}, in the methanol/water mixture is in the range of 0.5−0.8, the sizes of micelles are in the range of 20−30 nm in radius for *Py*-PNIPAM$_{50}$-*b*-POEGMA$_{18}$. At $\varphi_{water} = 0.5$, the formed micelles possess the highest overall micelle density and the largest molar mass. The effects of varying the block lengths of *Py*-PNIPAM-*b*-POEGMA diblock copolymers on the structural parameters of PNIPAM-core micelles have also been explored. Although we can observe the immediate appearance of bluish tinge upon mixing the diblock copolymer solution in methanol with equal volume of water ($\varphi_{water} = 0.5$), which is characteristic of the formation of micellar aggregates, the whole micellization process apparently takes a relatively long time to complete, as revealed by monitoring the time dependence of fluorescence emission spectra. The excimer/monomer fluorescence intensity ratios, I_E/I_M, continuously decrease with time and then reach a plateau value after ∼20 min. The decrease of I_E/I_M after the initial formation of pseudo-equilibrium micelles should be ascribed to the structural rearrangement and further packing of PNIPAM segments within the micelle core, restricting the mobility of pyrene end groups and decreasing the probability of contact between them. Compared to the conventional cosolvent approach employed for the micellization of block copolymers in selective solvents, the reported cononsolvency-induced unimer−micelle−unimer transition of *Py*-PNIPAM-*b*-POEGMA in methanol/water mixtures has been unprecedented.

Introduction

Amphiphilic block copolymers are self-assembling materials capable of forming polymeric micelles.[1] The driving force of micellization is generally attributed to the microphase precipitation of the insoluble block and the affinity of the soluble block to the solvent. Thus, the phase separation of the insoluble block is arrested at an early stage because of steric stabilization of the well-solvated block.[2−8] Following this principle, the selective alteration of the solubility of one block, such as interpolymer complexation,[9,10] chemical transformation,[11,12] stimuli-responsive solubility changes of double hydrophilic block copolymers,[13−21] and the addition of a selective solvent,[22−24] has been successfully employed to fabricate micellar nanoparticles possessing core−shell microstructures.[25] The approach of adding a selective solvent is widely employed for the micellization of an amphiphilic block copolymer with a relatively long insoluble block, which is also termed as the cosolvent method. A poor solvent selective to one of the blocks is added into the block copolymer solution in a common solvent to induce the micelle formation. Thus, with increasing volume fractions of the selective solvent, unimer-to-micelle transition can be typically observed.

* Corresponding author. E-mail: sliu@ustc.edu.cn.

(1) Riess, G. *Prog. Polym. Sci.* **2003**, *28*, 1107−1170.
(2) Harada, A.; Kataoka, K. *Macromolecules* **1995**, *28*, 5294−5299.
(3) Harada, A.; Kataoka, K. *Macromolecules* **1998**, *31*, 288−294.
(4) Yuan, X. F.; Yamasaki, Y.; Harada, A.; Kataoka, K. *Polymer* **2005**, *46*, 7749−7758.
(5) Kabanov, A. V.; Vinogradov, S. V.; Suzdaltseva, Y. G.; Alakhov, V. Y. *Bioconjugate Chem.* **1995**, *6*, 639−643.
(6) Kabanov, A. V.; Bronich, T. K.; Kabanov, V. A.; Yu, K.; Eisenberg, A. *Macromolecules* **1996**, *29*, 6797−6802.
(7) Gohy, J. F.; Varshney, S. K.; Antoun, S.; Jerome, R. *Macromolecules* **2000**, *33*, 9298−9305.
(8) Gohy, J. F.; Varshney, S. K.; Jerome, R. *Macromolecules* **2001**, *34*, 3361−3366.
(9) Topouza, D.; Orfanou, K.; Pispas, S. *J. Polym. Sci., Part A: Polym. Chem.* **2004**, *42*, 6230−6237.
(10) Zhang, W. Q.; Shi, L. Q.; Miao, Z. J.; Wu, K.; An, Y. L. *Macromol. Chem. Phys.* **2005**, *206*, 2354−2361.
(11) Chen, D. Y.; Peng, H. S.; Jiang, M. *Macromolecules* **2003**, *36*, 2576−2578.
(12) Wu, C.; Niu, A. Z.; Leung, L. M.; Lam, T. S. *J. Am. Chem. Soc.* **1999**, *121*, 1954−1955.
(13) Andre, X.; Zhang, M. F.; Muller, A. H. E. *Macromol. Rapid Commun.* **2005**, *26*, 558−563.
(14) Arotcarena, M.; Heise, B.; Ishaya, S.; Laschewsky, A. *J. Am. Chem. Soc.* **2002**, *124*, 3787−3793.
(15) Gohy, J. F.; Antoun, S.; Jerome, R. *Macromolecules* **2001**, *34*, 7435−7440.
(16) Rodriguez-Hernandez, J.; Lecommandoux, S. *J. Am. Chem. Soc.* **2005**, *127*, 2026−2027.
(17) Butun, V.; Billingham, N. C.; Armes, S. P. *J. Am. Chem. Soc.* **1998**, *120*, 11818−11819.
(18) Liu, S. Y.; Armes, S. P. *Angew. Chem., Int. Ed.* **2002**, *41*, 1413−1416.
(19) Liu, S. Y.; Armes, S. P. *Langmuir* **2003**, *19*, 4432−4438.
(20) Liu, S. Y.; Weaver, J. V. M.; Tang, Y. Q.; Billingham, N. C.; Armes, S. P.; Tribe, K. *Macromolecules* **2002**, *35*, 6121−6131.
(21) Liu, S. Y.; Billingham, N. C.; Armes, S. P. *Angew. Chem., Int. Ed.* **2001**, *40*, 2328.
(22) Antonietti, M.; Heinz, S.; Schmidt, M.; Rosenauer, C. *Macromolecules* **1994**, *27*, 3276−3281.
(23) Zhang, L. F.; Yu, K.; Eisenberg, A. *Science* **1996**, *272*, 1777−1779.
(24) Zhang, L. F.; Eisenberg, A. *Science* **1995**, *268*, 1728−1731.
(25) Voets, I. K.; de Keizer, A.; Stuart, M. A. C.; de Waard, P. *Macromolecules* **2006**, *39*, 5952−5955.

10.1021/la7020148 CCC: $37.00 © 2007 American Chemical Society
Published on Web 10/09/2007

Scheme 1. Reaction Scheme for the Preparation of *Py*-PNIPAM$_{50}$-*b*-POEGMA$_{18}$

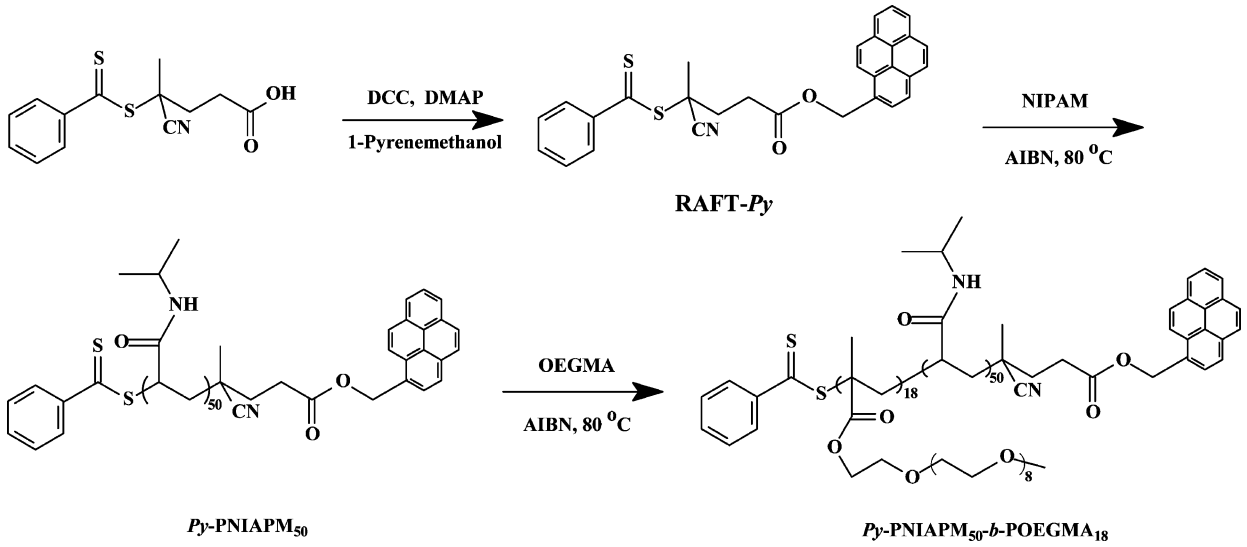

However, the solubility of mixed solvent to certain polymers is quite complex in some cases. Two intriguing types, cosolvency and cononsolvency, should be noted. Cosolvency is a modestly rare phenomenon, in which a mixture of two nonsolvents for a polymer becomes a good solvent. For example, methanol and water are nonsolvents for poly(methyl methacrylate) (PMMA), but a proper range of methanol/water mixture can molecularly dissolve PMMA.[26] On the other hand, even fewer examples exist for the reverse situation. A polymer is very soluble in two pure solvents separately, but it is insoluble in a mixture of them; this is called cononsolvency. Originally reported by Schild et al.,[27,28] poly(*N*-isopropylacrylamide) (PNIPAM) exhibits such rare solution properties in an appropriate mixture of water and polar organic solvents, such as methanol, ethanol, tetrahydrofuran, or dioxane. Winnik et al.[29−33] studied the cononsolvency-induced volume changes of fluorescently labeled PNIPAM gels and the phase transition behavior of PNIPAM chains. They successfully elucidated the preferential adsorption of organic solvent molecules surrounding the polymer chains. On the basis of the above analysis, we figured out that the cononsolvency properties of PNIPAM can be further utilized to fabricate micellar nanoparticles from PNIPAM-containing block copolymers. Moreover, cononsolvency-induced micellization of PNIPAM-containing block copolymers in solvent mixtures might exhibit the unique unimer−micelle−unimer transition behavior upon continuously changing solvent compositions.

On the other hand, most of the studies of block copolymer micelles focused on the characterization of their equilibrium structures, although in most cases it is uncertain whether the final equilibrium state has reached it or not. Like small molecule surfactants, the micellization kinetics of block copolymers is closely related to their stability, which plays an important role in various technological processes such as foaming, wetting, emulsification, solubilization, and detergency.[34,35] Our recent research interests involve the micellization processes (i.e., the kinetics of micelle formation).[36−39]

Herein, we synthesized pyrene end-labeled diblock copolymers, poly(*N*-isopropylacrylamide)-*b*-poly(oligo(ethylene glycol) methyl ether methacrylate) (*Py*-PNIPAM-*b*-POEGMA), via consecutive reversible addition-fragmentation chain transfer (RAFT) polymerization using a pyrene-containing dithioester as the RAFT agent (Scheme 1). In the current work, our goals are twofold. The first is to investigate the cononsolvency-induced unimer−micelle−unimer transition of *Py*-PNIPAM-*b*- EGMA diblock copolymers in methanol/water mixtures via a combination of ^{1}H NMR, laser light scattering (LLS), and transmission electron microscopy (TEM) techniques. Because the pyrene label located at the copolymer chain end is buried within PNIPAM-cores of micelles, our second goal is to explore the overall micellization process by monitoring the time dependence of excimer fluorescence intensity during the micellization of the diblock copolymer. To the best of our knowledge, this represents the first example of cononsolvency-induced micellization of chromophore end-labeled diblock copolymers (Scheme 2); moreover, the time scale of the whole micellization process has been investigated employing the quite sensitive fluorescence technique.

Experimental Section

Materials. *N*-Isopropylacrylamide (NIPAM) (97%, Tokyo Kasei Kagyo Co.) was purified by recrystallization from a mixture of benzene and *n*-hexane (1/3, v/v). 1-Pyrenemethanol and oligo(ethylene glycol) methyl ether methacrylate (OEGMA, M_n = 475, mean degree of polymerization, DP, is 8 to 9) were purchased from Aldrich. OEGMA monomer was purified by being passed through a neutral alumina column to remove the inhibitor. It was then stored at −20 °C before use. 1,4-Dioxane was distilled from CaH_2. 2,2′-Azobisisobutyronitrile (AIBN) was recrystallized from 95% ethanol.

(26) Cowie, J. M. G.; Mohsin, M. A.; McEwen, I. J. *Polymer* **1987**, *28*, 1569−1572.
(27) Schild, H. G.; Muthukumar, M.; Tirrell, D. A. *Macromolecules* **1991**, *24*, 948−952.
(28) Schild, H. G.; Tirrell, D. A. *J. Phys. Chem.* **1990**, *94*, 4352−4356.
(29) Winnik, F. M.; Ringsdorf, H.; Venzmer, J. *Macromolecules* **1990**, *23*, 2415−2416.
(30) Winnik, F. M.; Ottaviani, M. F.; Bossmann, S. H.; Garciagaribay, M.; Turro, N. J. *Macromolecules* **1992**, *25*, 6007−6017.
(31) Winnik, F. M.; Ottaviani, M. F.; Bossmann, S. H.; Pan, W. S.; Garciagaribay, M.; Turro, N. J. *Macromolecules* **1993**, *26*, 4577−4585.
(32) Asano, M.; Winnik, F. M.; Yamashita, T.; Horie, K. *Macromolecules* **1995**, *28*, 5861−5866.
(33) Ottaviani, M. F.; Winnik, F. M.; Bossmann, S. H.; Turro, N. J. *Helv. Chim. Acta* **2001**, *84*, 2476−2492.
(34) Patist, A.; Kanicky, J. R.; Shukla, P. K.; Shah, D. O. *J. Colloid Interface Sci.* **2002**, *245*, 1−15.
(35) Noskov, B. A. *Adv. Colloid Interface Sci.* **2002**, *95*, 237−293.
(36) Zhu, Z. Y.; Armes, S. P.; Liu, S. Y. *Macromolecules* **2005**, *38*, 9803−9812.
(37) Ge, Z. S.; Cai, Y. L.; Yin, J.; Zhu, Z. Y.; Rao, J. Y.; Liu, S. Y. *Langmuir* **2007**, *23*, 1114−1122.
(38) Wang, D.; Yin, J.; Zhu, Z. Y.; Ge, Z. S.; Liu, H. W.; Armes, S. P.; Liu, S. Y. *Macromolecules* **2006**, *39*, 7378−7385.
(39) Ge, Z. S.; Xie, D.; Chen, D. Y.; Jiang, X. Z.; Zhang, Y. F.; Liu, H. W.; Liu, S. Y. *Macromolecules* **2007**, *40*, 3538−3546.

Table 1. Structural Parameters of *Py*-PNIPAM-*b*-POEGMA Diblock Copolymers Prepared via RAFT Polymerizations

sample codes	DP of PNIPAM[a]	DP of POEGMA[a]	M_n[b]	M_w[b]	M_w/M_n[b]
Py-PNIPAM$_{75}$-*b*-POEGMA$_{50}$	75	50	36 300	41 700	1.15
Py-PNIPAM$_{75}$-*b*-POEGMA$_{38}$	75	38	31 600	35 400	1.12
Py-PNIPAM$_{75}$-*b*-POEGMA$_{20}$	75	20	22 500	24 300	1.08
Py-PNIPAM$_{50}$-*b*-POEGMA$_{31}$	50	31	23 900	27 200	1.14
Py-PNIPAM$_{50}$-*b*-POEGMA$_{18}$	50	18	14 500	15 800	1.09

[a] Determined by ^{1}H NMR in $CDCl_3$. [b] Determined by GPC using THF as the eluent.

Scheme 2. Schematic Illustration of Cononsolvency-Induced Micellization Behavior of *Py*-PNIPAM$_{50}$-*b*-POEGMA$_{18}$ Diblock Copolymer in Methanol/Water Mixture

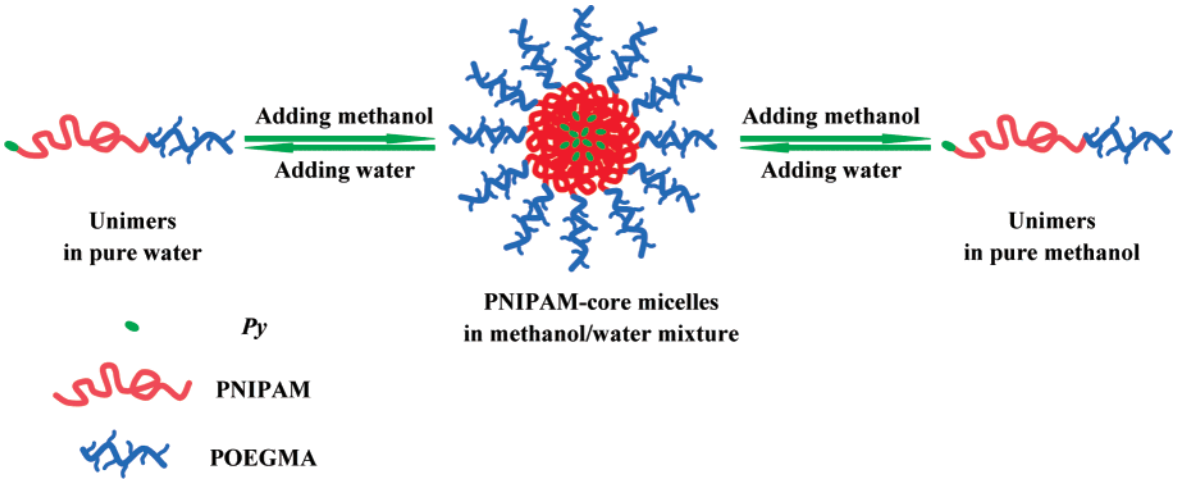

4-Cyano-4-(thiobenzoyl)sulfanyl pentanoic acid was synthesized following literature procedures.[40] All other chemicals were purchased from Shanghai Chemical Reagent Co. and used as received.

Sample Preparation. General approaches to the preparation of 4-cyano-4-(thiobenzoyl)sulfanyl pentanoic pyrenemethyl ester (RAFT-*Py*), *Py*-PNIPAM, and *Py*-PNIAPM-*b*-POEGMA diblock copolymers are shown in Scheme 1.

Preparation of RAFT-Py. 4-Cyano-4-(thiobenzoyl)sulfanyl pentanoic acid (1.40 g, 5.0 mmol) and 1-pyrenemethanol (1.16 g, 5.0 mmol) were dissolved in 20 mL of $CHCl_3$, followed by the addition of *N*,*N*′-dicyclohexylcarbodiimide (DCC) (1.03 g, 5.0 mmol) and 4-dimethylaminopyridine (DMAP) (0.06 g, 0.5 mmol).[41,42] The reaction mixture was stirred at 0 °C for 24 h. After filtration, the filtrate was concentrated under reduced pressure. The crude product was purified by column chromatography using CH_2Cl_2 as eluent to yield 1.43 g (~60% yield) of RAFT-*Py*. The resulting product was dried overnight in a vacuum oven at 25 °C. ^{1}H NMR ($CDCl_3$, δ): 7.8−8.4 (9H, $C_{16}H_9$), 7.2−7.6 (5H, C_6H_5), 5.9 (2H, $CH_2C_{16}H_9$), 2.3−2.8 (4H, CH_2CH_2OCO), 1.9 (3H, CH_3C).

Synthesis of Py-PNIPAM macroRAFT Agent. RAFT polymerization was used to prepare *Py*-PNIPAM macroRAFT agent and the *Py*-PNIPAM-*b*-POEGMA diblock copolymer (Scheme 1). A typical procedure for the synthesis of *Py*-PNIPAM$_{50}$ macroRAFT agent was as follows. NIPAM (0.45 g, 4.0 mmol), RAFT-*Py* (0.02 g, 0.05 mmol), and AIBN (1.6 mg, 0.01 mmol) at the molar ratio of 400:5:1 were charged into a glass ampule containing 3 mL of 1,4-dioxane. The mixture was degassed through three freeze−thaw cycles. The ampule was then flame sealed under vacuum and kept in an oil bath preheated at 80 °C to conduct the polymerization. After 12 h, the ampule was put into liquid nitrogen to stop the polymerization. The reaction mixture was diluted with 3 mL of THF and precipitated into an excess of diethyl ether. This purification cycle was repeated twice. The obtained slightly pink powder was dried in a vacuum oven overnight at room temperature. The molecular weight and molecular weight distribution of PNIPAM homopolymer were determined by gel permeation chromatography (GPC) using THF as eluent: M_n = 7600, M_w/M_n = 1.07. The actual DP of *Py*-PNIPAM was determined to be 50 by ^{1}H NMR analysis in $CDCl_3$. The obtained macroRAFT agent was denoted *Py*-PNIPAM$_{50}$. Another *Py*-PNIPAM macroRAFT agent with a DP of 75, *Py*-PNIPAM$_{75}$, was prepared according to similar procedures described earlier, and GPC analysis gave an M_n of 12 100 and an M_w/M_n of 1.14.

Synthesis of Py-PNIPAM-b-POEGMA Diblock Copolymer. In a typical run for the synthesis of *Py*-PNIPAM$_{50}$-*b*-POEGMA$_{18}$, *Py*-PNIPAM (0.31 g, 0.05 mmol), OEGMA (0.48 g, 1.0 mmol), and AIBN (1.7 mg, 0.01 mmol) at the molar ratio of 5:100:1 were charged into a glass ampule containing 3 mL of 1,4-dioxane. The mixture was degassed via three freeze−thaw cycles. The ampule was then sealed under vacuum and kept in an oil bath preheated at 80 °C to conduct the polymerization. After 16 h, the ampule was put into liquid nitrogen to stop the polymerization. The reaction mixture was diluted with 3 mL of THF and then precipitated into an excess of diethyl ether. This purification cycle was repeated twice. The obtained viscous solid (0.58 g, 73% yield) was dried in a vacuum oven overnight at room temperature. The molecular weight and molecular weight distribution of *Py*-PNIPAM-*b*-POEGMA diblock copolymer were determined by GPC using THF as eluent: M_n = 14 500, M_w/M_n = 1.09. The DP of the POEGMA block was determined to be 18 by ^{1}H NMR in $CDCl_3$. The obtained diblock copolymer was denoted *Py*-PNIPAM$_{50}$-*b*-POEGMA$_{18}$. According to similar procedures, other pyrene end-labeled diblock copolymers with varying block lengths were also synthesized, and their structural parameters are summarized in Table 1.

Characterization. *Nuclear Magnetic Resonance Spectroscopy.* All ^{1}H NMR spectra were performed at 25 °C on a Bruker AV300 NMR spectrometer (resonance frequency of 300 MHz for ^{1}H) operating in the Fourier transform mode.

Gel Permeation Chromatography. Molecular weights and molecular weight distributions were determined by GPC equipped with Waters 1515 pump and Waters 2414 differential refractive index detector (set at 30 °C). It uses a series of three linear Styragel columns HT2, HT4, and HT5 at an oven temperature of 45 °C. The eluent

(40) Thang, S. H.; Chong, Y. K.; Mayadunne, R. T. A.; Moad, G.; Rizzardo, E. *Tetrahedron Lett.* **1999**, *40*, 2435−2438.
(41) Zhou, N.; Lu, L.; Zhu, J.; Yang, X.; Wang, X.; Zhu, X.; Zhang, Z. *Polymer* **2007**, *48*, 1255−1260.
(42) Chen, M.; Ghiggino, K. P.; Mau, A. W. H.; Rizzardo, E.; Thang, S. H.; Wilson, G. J. *Chem. Commun.* **2002**, 2276−2277.

was THF at a flow rate of 1.0 mL/min. A series of low polydispersity polystyrene standards were employed for the GPC calibration.

Laser Light Scattering. The dynamic and static LLS measurements were performed at 25 °C on a commercial spectrometer (ALV/DLS/SLS-5022F) equipped with a multi-τ digital time correlator (ALV5000) and a cylindrical 22 mW UNIPHASE He−Ne laser (λ_0 = 632 nm) as the light source. The measurements were conducted ~1 h after mixing the copolymer solution in methanol with water. All solutions were clarified by 0.45-μm Millipore nylon filters.

In dynamic LLS, scattered light was collected at a fixed angle of 15° for a duration of 10 min. Distribution averages and particle size distributions were computed using cumulants analysis and CONTIN routines. All data were averaged over three measurements.

In static LLS, we can obtain the weight-average molar mass (M_w) and the *z*-average root-mean square radius of gyration ($\langle R_g^2\rangle^{1/2}$ or written as $\langle R_g\rangle$) of nanoparticles from the angular dependence of the excess absolute scattering intensity, known as the Rayleigh ratio $R_{vv}(q)$, as

$$\frac{KC}{R_{vv}(q)} \approx \frac{1}{M_w}\left(1 + \frac{1}{3}\langle R_g^2\rangle q^2\right) + 2A_2C \qquad (1)$$

where $K = 4\pi^2 n^2 (dn/dC)^2/(N_A\lambda_0^4)$ and $q = (4\pi n/\lambda_0)\sin(\theta/2)$ with N_A, dn/dC, n, and λ_0 being the Avogadro number, the specific refractive index increment, the solvent refractive index, and the wavelength of the laser light in a vacuum, respectively; and A_2 is the second virial coefficient. For the determination of absolute molar masses ($M_{w,LLS}$) of PNIPAM-core micelles, Zimm plots were established over 13 angles (30−90°) in the concentration range of 0.05−0.5 g/L. Refractive indexes (n) of methanol/water mixtures and refractive index increments (dn/dC) of *Py*-PNIPAM-*b*-POEGMA in methanol/water mixtures at different φ_{water} were determined by an Abbe refractometer and a precise differential refractometer at the same wavelength of 632 nm,[43] respectively. dn/dC values are listed in Tables S1 and S2 (Supporting Information).

Fluorescence Spectroscopy. Fluorescence spectra were recorded using a Shimadzu RF-5301PC spectrofluorometer. The temperature of the water-jacketed cell holder was controlled at 25 °C by a programmable circulation bath. The excitation and emission slit widths were set at 7.5 and 2.5 nm, respectively. The time dependence of the ratio of the emission intensity at 480 nm to that at 373 nm, I_E/I_M, was employed to monitor the micellization process, time-resolved fluorescence emission spectra were recorded every 20 s, and the spectra scanning rate was set at 1000 nm/min.

Transmission Electron Microscopy. TEM observations were conducted on a Philips CM 120 electron microscope at an acceleration voltage of 100 kV. The sample for TEM observations was prepared by placing 10 μL of micelle solutions at a concentration of 0.1 g/L on copper grids, which were coated with thin films of Formvar and carbon successively. No staining was required.

Results and Discussion

Synthesis of *Py*-PNIPAM and *Py*-PNIPAM-*b*-POEGMA. The general approaches employed for the preparation of *Py*-PNIPAM macroRAFT agents and *Py*-PNIPAM-*b*-POEGMA diblock copolymers are shown in Scheme 1. The target block copolymers were synthesized by consecutive RAFT polymerizations of NIPAM and OEGMA monomers.

Synthesis of Py-PNIPAM macroRAFT Agent. The pyrene-containing RAFT agent, RAFT-*Py*, was synthesized by coupling 4-cyano-4-(thiobenzoyl)sulfanyl pentanoic acid and 1-pyrenemethanol in the presence of DCC and DMAP as the catalysts. Figure 1a shows the ^{1}H NMR spectrum of RAFT-*Py* and the corresponding peak assignments. The signals at δ = 7.2−7.6 and 7.8−8.4 ppm are ascribed to the phenyl and pyrene groups, respectively. The signals at δ = 5.9, 2.3−2.8, and 1.9 ppm are attributed to the protons of three methylene groups (d, c, f) and methyl group (b), respectively.

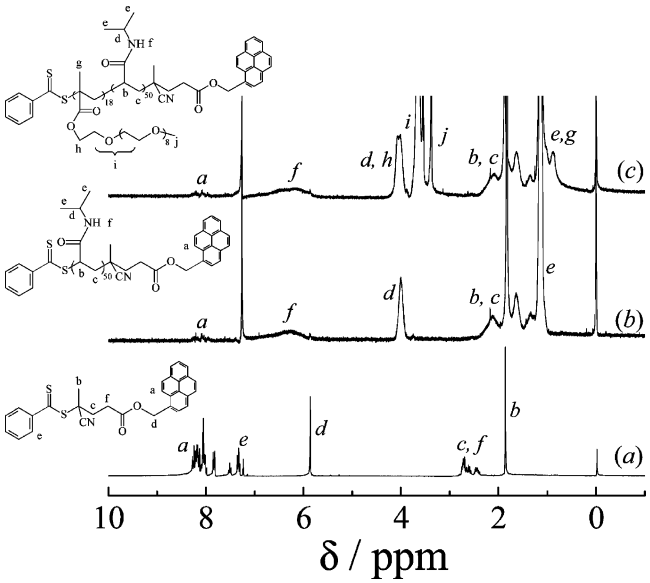

Figure 1. ^{1}H NMR spectra of (a) RAFT-*Py*, (b) *Py*-PNIPAM$_{50}$ macroRAFT agent, and (c) *Py*-PNIPAM$_{50}$-*b*-POEGMA$_{18}$ in $CDCl_3$.

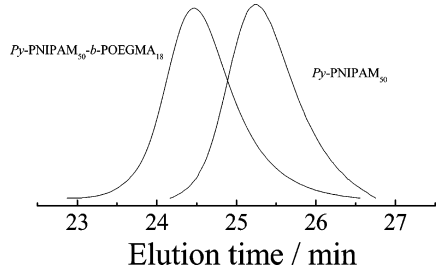

Figure 2. GPC traces of *Py*-PNIPAM$_{50}$ macroRAFT agent and *Py*-PNIPAM$_{50}$-*b*- POEGMA$_{18}$.

NIPAM was polymerized at 80 °C using RAFT-*Py* as the mediating agent. The ^{1}H NMR spectrum in Figure 1b reveals the presence of signals characteristic of PNIPAM at δ = 5.8−7.0, 4.0, and 1.2 ppm. Signals at δ = 7.8−8.4 ppm are ascribed to the pyrene group located at the PNIPAM chain end. GPC analysis in THF reveals a monomodal and symmetric peak with $M_n \approx$ 7600 and a polydispersity, M_w/M_n, of 1.07. The actual DP of *Py*-PNIPAM was determined to be 50 on the basis of comparison of the integration areas of peaks d and a. *Py*-PNIPAM$_{75}$ with M_n of 12 100 and M_w/M_n of 1.14 was also prepared according to similar procedures.

Synthesis of Py-PNIPAM-b-POEGMA. The obtained *Py*-PNIPAM homopolymers were then employed as macroRAFT agents to polymerize OEGMA monomer, leading to the formation of *Py*-PNIPAM-*b*-POEGMA diblock copolymers. ^{1}H NMR spectrum of the final product (Figure 1c) revealed the presence of signals from both PNIPAM and POEGMA blocks. Most importantly, GPC traces in Figure 2 clearly showed that the elution peak shifts to higher molecular weight after block copolymerization of OEGMA. The diblock copolymer elution peak is relatively symmetric, confirming the almost complete consumption of macroRAFT agent. The DP of the POEGMA block was determined to be 18 by ^{1}H NMR. The obtained diblock copolymer was denoted as *Py*-PNIPAM$_{50}$-*b*-POEGMA$_{18}$. The molecular weight and molecular weight distribution were characterized by GPC analysis in THF: M_n = 14 500, M_w/M_n = 1.09. Other *Py*-PNIPAM-*b*-POEGMA diblock copolymer

(43) Wu, C.; Xia, K. Q. *Rev. Sci. Instrum.* **1994**, *65*, 587−590.

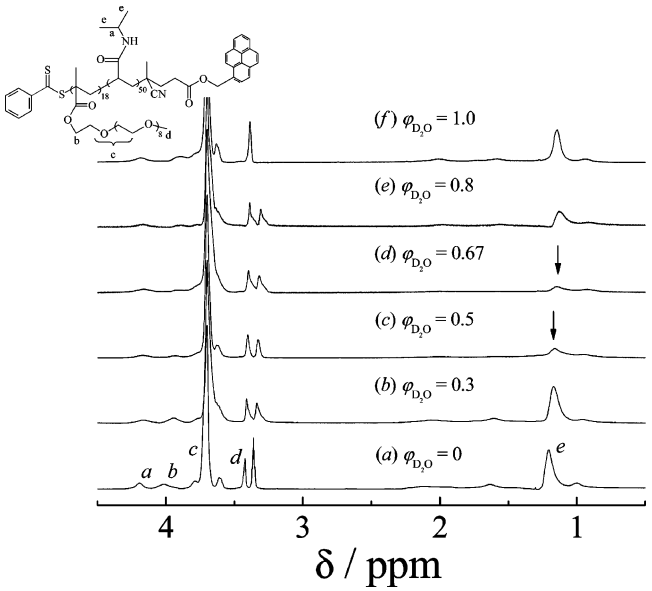

Figure 3. ^{1}H NMR spectra of *Py*-PNIPAM$_{50}$-*b*-POEGMA$_{18}$ in a CD_3OD/D_2O mixture at different φ_{D_2O}. From bottom to top, φ_{D_2O} = 0, 0.3, 0.5, 0.67, 0.8, and 1.0, respectively.

samples were obtained following similar procedures described earlier, and their structural parameters are summarized in Table 1.

Although the GPC trace of *Py*-PNIPAM$_{50}$-*b*-POEGMA$_{18}$ is relatively symmetric, we cannot exclude the possible presence of residual PNIPAM homopolymer in the final product, which is intrinsic of the mechanism of the RAFT process. Considering that a shoulder peak at the lower molecular weight side was not observed in the GPC trace of the diblock copolymer (Figure 2), the relative content of PNIPAM homopolymer in the diblock copolymer should be quite low (<5 wt %). In subsequent cononsolvency-induced micellization studies, if present, residual PNIPAM homopolymer will locate within PNIPAM cores of the formed micelles, and further discussion of their effects on the structural parameters of PNIPAM-core micelles was not attempted.

Cononsolvency-Induced Micellization of *Py*-PNIPAM$_{50}$-*b*-POEGMA$_{18}$. *^{1}H NMR Studies.* Dye solubilization, fluorescence, and LLS techniques have been frequently employed to monitor the onset of micellization and characterize the micelle microstructures.[44−47] As chain segments in the micelle core possess decreased chain mobility compared to that of free chains, ^{1}H NMR can also be conveniently utilized to study the micellization of stimuli-responsive block copolymers, providing the structural information of which block sequence in the copolymer is forming the micellar core.[45,48−51]

Figure 3 shows the ^{1}H NMR spectra of *Py*-PNIPAM$_{50}$-*b*-POEGMA$_{18}$ at six different volume fractions of D_2O, φ_{D_2O}, in CD_3OD/D_2O solvent mixtures. The signals at δ = 1.2 and 3.7 ppm are characteristic of the PNIPAM and POEGMA blocks, respectively (see peak assignments in Figure 1c). In pure CD_3OD or D_2O (Figure 3a,f), characteristic signals due to both blocks can be clearly seen, and all signals remain relatively sharp, indicating that the diblock copolymer molecularly dissolves. At φ_{D_2O} = 0.3 (Figure 3b), the relative intensity of signal characteristic of PNIPAM at 1.2 ppm remains unchanged; moreover, the integral ratio of the peak at δ = 1.2 to that at δ = 3.7 ppm is the same as that obtained for *Py*-PNIPAM$_{50}$-*b*-POEGMA$_{18}$ in $CDCl_3$ (Figure 1c). This confirms that the PNIPAM block still remains soluble at φ_{D_2O} = 0.3.

Upon further increasing φ_{D_2O} to 0.5 and 0.67 (Figure 3c,d), the relative intensity of characteristic PNIPAM signal at 1.2 ppm decreases considerably, indicating that the PNIPAM block gets insoluble because of cononsolvency. On the other hand, the characteristic signals of the POEGMA block are clearly evident, which is reasonable as the POEGMA block remains soluble in the whole range of solvent mixture. On the basis of chemical intuition, PNIPAM-core micelles stabilized with POEGMA corona should form (Scheme 2).

At φ_{D_2O} = 0.8 (Figure 3e), the relative intensity of characteristic PNIPAM signal at 1.2 ppm to that of POEGMA increases a little bit, but still much lower than that in pure CD_3OD or D_2O. This indicates that, at φ_{D_2O} = 0.8, the extent of solvation of the PNIPAM block is getting higher compared to that at φ_{D_2O} = 0.5 and 0.67. Thus, PNIPAM-core micelles with relatively loose structures should form φ_{D_2O} = 0.8. This argument will be further corroborated by subsequent LLS and fluorescence studies.

PNIPAM homopolymer exhibits cononsolvency behavior in methanol/water mixture when the volume of water, φ_{water}, is in the range of 0.35−0.85 at 25 °C.[29,30,52] The φ_{D_2O} range in which we observe the suppression of PNIPAM signals by ^{1}H NMR (i.e., the cononsolvency-induced micellization) is in general agreement with those reported for PNIPAM hompolymers.

It should be noted that, even at φ_{D_2O} = 0.5 and 0.67, the characteristic PNIPAM signals do not completely disappear, suggesting that the PNIPAM block remains partially solvated (i.e., the micelle core still contains relatively large amounts of solvent molecules). This is similar to the case of thermoresponsive micellization of poly(propylene oxide)- or PNIPAM-containing block copolymers.[45,50,51] Hurter et al.[53] also theoretically predicted the presence of water in the micellar core in their modeling of the thermo-induced micellization of Pluronics. Wang et al.[54] reported that, for PNIPAM homopolymer, its single chain globule still contains ∼66% water even in the fully collapsed state. In contrast, in previous studies of the pH-induced micellization of poly(hexa(ethylene glycol) methacrylate)-*b*-poly(2-(diethylamino)ethyl methacrylate), PHEGMA-*b*-PDEA, ^{1}H NMR of PDEA-core micelles did not reveal any peaks assignable to the PDEA residues.[48] This suggests that this latter system possesses a much more hydrophobic core.

Laser Light Scattering Characterization. Dynamic and static LLS were then employed to characterize the cononsolvency-induced formation of PNIPAM-core micelles, stabilized by the soluble POEGMA corona. Figure 4 shows typical hydrodynamic radius distributions, $f(R_h)$, of *Py*-PNIPAM$_{50}$-*b*-POEGMA$_{18}$ in methanol/water mixture at different volume fractions of water, φ_{water}. At φ_{water} = 0 and 1.0, the average hydrodynamic radii, $\langle R_h \rangle$, are ∼6−8 nm and the scattered light intensity is quite low, confirming that the diblock copolymer molecularly dissolves.

(44) Qiu, X. P.; Wu, C. *Macromolecules* **1997**, *30*, 7921−7926.
(45) Nivaggioli, T.; Tsao, B.; Alexandridis, P.; Hatton, T. A. *Langmuir* **1995**, *11*, 119−126.
(46) Alexandridis, P.; Holzwarth, J. F.; Hatton, T. A. *Macromolecules* **1994**, *27*, 2414−2425.
(47) Patrickios, C. S.; Forder, C.; Armes, S. P.; Billingham, N. C. *J. Polym. Sci., Part A: Polym. Chem.* **1996**, *34*, 1529−1541.
(48) Vamvakaki, M.; Palioura, D.; Spyros, A.; Armes, S. P.; Anastasiadis, S. H. *Macromolecules* **2006**, *39*, 5106−5112.
(49) Forder, C.; Patrickios, C. S.; Armes, S. P.; Billingham, N. C. *Macromolecules* **1996**, *29*, 8160−8169.
(50) Cau, F.; Lacelle, S. *Macromolecules* **1996**, *29*, 170−178.
(51) Wanka, G.; Hoffmann, H.; Ulbricht, W. *Macromolecules* **1994**, *27*, 4145−4159.
(52) Zhang, G. Z.; Wu, C. *J. Am. Chem. Soc.* **2001**, *123*, 1376−1380.
(53) Hurter, P. N.; Scheutjens, J. M. H. M.; Hatton, T. A. *Macromolecules* **1993**, *26*, 5030−5040.
(54) Wang, X. H.; Qiu, X. P.; Wu, C. *Macromolecules* **1998**, *31*, 2972−2976.

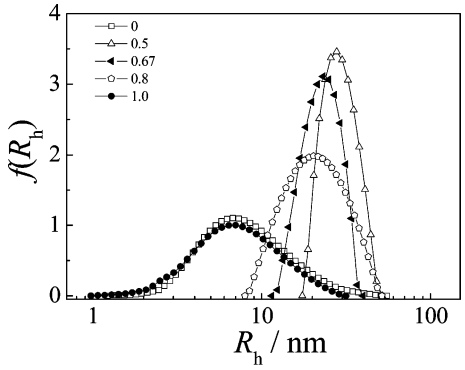

Figure 4. Hydrodynamic radius distributions, $f(R_h)$, of *Py*-PNIPAM$_{50}$-*b*-POEGMA$_{18}$ in methanol/water mixture at different φ_{water} values.

As φ_{water} increases to the range of 0.5−0.8, the solution exhibits a bluish tinge, which is characteristic of micellar solutions. It should be noted that the dispersion is stable for more than three months. Dynamic LLS reveals relatively narrow size distributions, with average hydrodynamic radius, $\langle R_h \rangle$, in the range of 20−30 nm. This indicates the formation of core−shell nanoparticles due to the cononsolvency of PNIPAM block (Scheme 2).

It should be noted that, at $\varphi_{water} = 0.5$, the formed PNIPAM-core micelles possess the narrowest size distribution, with typical polydispersities (μ_2/Γ^2) less than 0.1 (Table 2). As φ_{water} increases to 0.67 and 0.8, the size distribution gets a little broader, and we can clearly observe a shift of average micelle size to smaller values, with $\langle R_h \rangle$ being 23 and 20 nm, respectively.

Figure 5 shows the variation of $\langle R_h \rangle$ and the micelle molar mass, $M_{w,LLS}$, as a function of φ_{water}. We can see that as φ_{water} increases from 0 to 0.3, $\langle R_h \rangle$ stays almost unchanged, indicating the absence of micelle formation. In the final φ_{water} range of 0.5−0.8, $\langle R_h \rangle$ is in the range 20−30 nm, showing a maximum at $\varphi_{water} = 0.5$ (Figure 5a), suggesting the cononsolvency-induced formation of PNIPAM-core micelles. This is in agreement with the conclusion obtained from previous ^{1}H NMR results. Upon further increasing φ_{water} to >0.8, the PNIPAM block gets soluble again, and the block copolymer molecularly dissolves, giving a $\langle R_h \rangle$ values close to the unimer state (Scheme 2).

In the φ_{water} range of 0.5−0.8, the obtained $M_{w,LLS}$ values are much larger than that in pure methanol or water (Figure 5b). The variation of $M_{w,LLS}$ with φ_{water} follows trends similar to that of $\langle R_h \rangle$, and we can observe a local $M_{w,LLS}$ maximum at $\varphi_{water} = 0.5$.

Table 2 summarizes the LLS characterization results of the micelles of *Py*-PNIPAM$_{50}$-*b*-POEGMA$_{18}$ at three different φ_{water}. The average aggregation numbers per micelle (N_{agg}) are estimated to be 750, 310, and 150 at φ_{water} of 0.5, 0.67, and 0.8, respectively. Using the equation $\rho = M_{w,LLS}/(4\pi/3N_a\langle R_h \rangle^3)$, we estimate the micelle densities, $\langle \rho \rangle$, at $\varphi_{water} = 0.5$ and 0.67 to be 0.22 and 0.16 g/mL, respectively. At $\varphi_{water} = 0.8$, the average micelle density is calculated to be 0.12 g/mL. It should be noted that the average micelle densities in all cases are relatively low compared to the bulk density of the copolymer, indicating that the micelle core still contains a large amount of solvent molecules and POEGMA blocks in the micelle corona are highly swollen. This is also in agreement with the ^{1}H NMR results, in which signals due to the PNIPAM block can be discerned at all φ_{water} values.

From Table 2, we can also observe that $\langle R_g \rangle/\langle R_h \rangle$ ratios of the cononsolvency-induced micelles decrease from 1.15 at $\varphi_{water} = 0.8$ to 0.71 at $\varphi_{water} = 0.5$. The latter is close to the theoretical value of 0.774, predicted for a nondraining hard sphere.[55] At $\varphi_{water} = 0.5$, the formed PNIPAM-core micelles possess the highest average micelle density and the lowest $\langle R_g \rangle/\langle R_h \rangle$, indicating a relatively compact micelle structure. At $\varphi_{water} = 0.8$, the micelle density is the lowest, indicating a relatively loose micelle structure; this also agrees well with ^{1}H NMR results (Figure 3). It is worth noting that thermoresponsive micellization behavior of poly(ethylene oxide)-*b*-poly(*N*-isopropylacrylamide) (PEO-*b*-PNIPAM), which is structurally similar to *Py*-PNIPAM$_{50}$-*b*-POEGMA$_{18}$, has been extensively investigated, taking advantage of the well-known lower critical solution temperature phase behavior of PNIPAM block.[56−58]

The formation of PNIPAM-core micelles has been further confirmed by TEM observations. Figure 6 gives typical TEM images of micelles formed from *Py*-PNIPAM$_{50}$-*b*-POEGMA$_{18}$ diblock copolymer in methanol/water mixtures at $\varphi_{water} = 0.5$ and 0.8, respectively (Figure 6). Both of them reveal the presence of spherical nanoparticles. PNIPAM-core micelles formed at $\varphi_{water} = 0.5$ apparently possess narrower size distributions as compared to that at $\varphi_{water} = 0.8$.

Dynamic and static LLS characterization results of micelles formed at $\varphi_{water} = 0.5$ from other *Py*-PNIPAM-*b*-POEGMA diblock copolymers (Table 1) are summarized in Table 3. Block copolymers with longer PNIPAM blocks typically form larger micelles. It should also be noted that $\langle R_g \rangle/\langle R_h \rangle$ ratios of PNIPAM-core micelles are in the range of 0.68−0.80, which are close to the theoretical value of 0.774, predicted for nondraining hard spheres.[55] For block copolymers with the same PNIPAM block length, $\langle R_h \rangle$ and $\langle N_{agg} \rangle$ values typically decrease with increasing DP of the soluble POEGMA block. The variation of micelle sizes and average aggregation numbers with the relative block length ratios of block copolymers has been well-documented in the literature.[1]

Micellization Process Studied by Fluorescence Spectroscopy. The above ^{1}H NMR, LLS, and TEM results all confirmed the cononsolvency-induced formation of PNIPAM-core micelles stabilized by the POEGMA corona in the methanol/water mixture with φ_{water} in the range of 0.5−0.8. However, these three techniques only give equilibrium structural information of the formed micelles. Taking advantage of the pyrene probe covalently attached at the copolymer chain end, the cononsolvency-induced micellization process of *Py*-PNIPAM-*b*-POEGMA can be further explored by time-resolved fluorescence spectroscopy.

Pyrene has been widely used as a probe of structure and dynamics in macromolecular systems because of its long excited-state lifetime and spectral sensitivity to the surrounding medium. Excimer fluorescence measurements of the excimer-to-monomer intensity ratio (I_E/I_M) provide highly localized information because the excimer is only formed when aromatic rings closely approach each other within 4−5 Å.[59−61]

In preliminary fluorescence experiments, we found that among the five diblock copolymers listed in Table 1, *Py*-PNIPAM$_{50}$-*b*-POEGMA$_{18}$ gives the strongest excimer emission peak after micellization, whereas the other four block copolymers exhibit

(55) Teraoka, I. *Polymer Solutions: An Introduction to Physical Properties;* Wiley & Sons: New York, 2002.
(56) Zhang, W. Q.; Shi, L. Q.; Wu, K.; An, Y. G. *Macromolecules* **2005**, *38*, 5743−5747.
(57) Virtanen, J.; Holappa, S.; Lemmetyinen, H.; Tenhu, H. *Macromolecules* **2002**, *35*, 4763−4769.
(58) Motokawa, R.; Morishita, K.; Koizumi, S.; Nakahira, T.; Annaka, M. *Macromolecules* **2005**, *38*, 5748−5760.
(59) Winnik, F. M. *Macromolecules* **1990**, *23*, 233−242.
(60) Chen, W.; Durning, C. J.; Turro, N. J. *Macromolecules* **1999**, *32*, 4151−4153.
(61) Kalyanasundaram, K.; Thomas, J. K. *J. Am. Chem. Soc.* **1977**, *99*, 2039−2044.

Table 2. Dynamic and Static LLS Characterization of PNIPAM-Core Micelles Formed from *Py*-PNIPAM$_{50}$-*b*-POEGMA$_{18}$ Diblock Copolymer at Different φ_{water} Values

φ_{water}	$M_{w,LLS}$[a] (g/mol)	$\langle R_h \rangle$[b] (nm)	$\langle R_g \rangle$[b] (nm)	$\langle R_g \rangle / \langle R_h \rangle$	N_{agg}[c]	ρ[d] (g/mL)	μ_2/Γ^2
0.5	1.2×10^7	28	20	0.71	750	0.22	0.097
0.67	4.9×10^6	23	21	0.91	310	0.16	0.173
0.8	2.4×10^6	20	23	1.15	150	0.12	0.155

[a] The absolute molar masses of PNIPAM-core micelles determined by static LLS via Zimm plots in the concentration range of 0.05−0.5 g/L. [b] Determined by dynamic and static LLS; the estimated error associated with each value was ±2 nm. [c] Calculated as: $N_{agg} = M_{w,LLS}/M_w$, where M_w is the weight-average molecular weight of the *Py*-PNIPAM$_{50}$-*b*-POEGMA$_{18}$ chain. [d] Calculated as: $\rho = M_{w,LLS}/(4\pi/3N_A\langle R_h \rangle^3)$, where N_A is the Avogadro number.

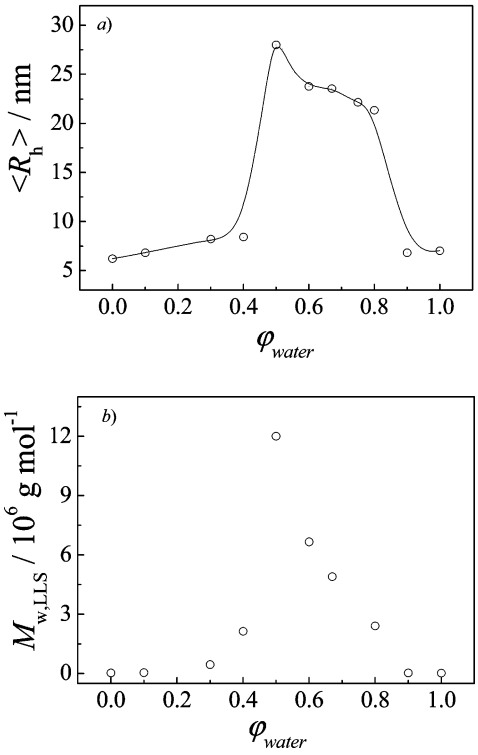

Figure 5. Variation of (a) intensity-average hydrodynamic radius, $\langle R_h \rangle$, and (b) absolute molar masses, $M_{w,LLS}$, of cononsolvency-induced PNIPAM-core micelles of *Py*-PNIPAM$_{50}$-*b*-POEGMA$_{18}$ in methanol/water mixture as a function of φ_{water}.

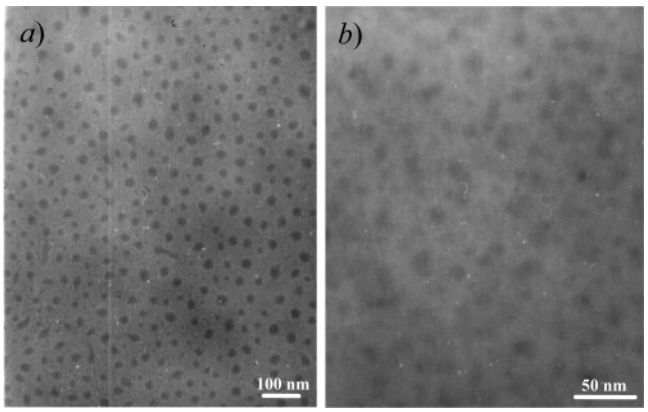

Figure 6. TEM images of PNIPAM-core micelles formed from *Py*-PNIPAM$_{50}$-*b*-POEGMA$_{18}$ at φ_{water} values of (a) 0.5 and (b) 0.8.

relatively weak excimer emissions, probably due to the much lower pyrene contents. Thus, the subsequent fluorescence characterization concentrates on *Py*-PNIPAM$_{50}$-*b*-POEGMA$_{18}$.

During the characterization of cononsolvency-induced micelle formation by fluorescence spectroscopy, we discovered that the I_E/I_M values change with time for freshly prepared micellar solution, although we can observe immediate appearance of the bluish tinge, which is characteristic of micellar aggregates, upon mixing the diblock copolymer solution in methanol with equal volume of water ($\varphi_{water} = 0.5$). We then realized that the change of I_E/I_M with time actually can be used to monitor the micellization process. It is worth noting that the time scale of the micellization processes of block copolymers has remained less explored in previous reports.

Figure 7 shows typical fluorescence spectra of *Py*-PNIPAM$_{50}$-*b*-POEGMA$_{18}$ in a methanol/water mixture at $\varphi_{water} = 0.5$, where the time interval between each spectrum was 5 min. The first spectrum was recorded ∼5 s after mixing. In addition to the monomer bands that are characteristic of the pyrene vibronic structure, which exhibits three distinct peaks at 373, 393, and 415 nm, the excimer emission of pyrene appears as a broad, structureless band around 480 nm. The spectral parameter of interest to us is the excimer (480 nm) to monomer (373 nm) intensity ratio, I_E/I_M. Figure 8 depicts the time dependence of I_E/I_M for *Py*-PNIPAM$_{50}$-*b*-POEGMA$_{18}$ in a methanol/water mixture at $\varphi_{water} = 0.5$, where the time intervals between each point were 20 s. It is quite evident that I_E/I_M decreases continuously with time and stabilizes out after ∼20 min. Single-exponential fitting of the dynamic curve results in a characteristic relaxation time of ∼420 s.

Previously, we have studied the pH-induced micellization kinetics of a poly(glycerol monomethacrylate)-*b*-poly(2-(dimethylamino)ethyl methacrylate)-*b*-poly(2-(diethylamino)ethyl methacrylate) (PGMA-*b*-PDMA-*b*-PDEA) triblock copolymer via the stopped-flow light scattering technique.[36] Upon jumping from pH 4 to pH > 8, we can observe a relaxation process with positive amplitude. The relaxation curve can be well fitted with a double exponential function, leading to a fast relaxation time constant (τ_1) and a slow relaxation time constant (τ_2). τ_1 is in the range of 10−20 ms, which is associated with the quick association of unimers into quasi-equilibrium micelles. τ_2 is around 110 ms, which is related to the micelle formation and breakup, approaching the final equilibrium micelles. It should be noted that the stopped-flow results only reflect the early stages of the micellization kinetics.

Recently, Nyrkova and Semenov[62,63] proposed theoretically that the unimer-to-micelle transition cannot be characterized by just two relaxation times, but rather by a continuous spectrum of relaxation times, owing to increasing energy barrier with growing micelle aggregation numbers. Most importantly, the growing micelles therefore may never reach the near-equilibrium size, and their growth may be arrested at an intermediate stage.

In the current case, the early stage kinetics is missing, as the first point is obtained ∼5 s after the changes of solvent quality to cononsolvency conditions. Thus, the continual decrease of I_E/I_M observed with time-resolved fluorescence spectroscopy (τ

(62) Nyrkova, I. A.; Semenov, A. N. *Macromol. Theory Simul.* **2005**, *14*, 569−585.
(63) Nyrkova, I. A.; Semenov, A. N. *Faraday Discuss.* **2005**, *128*, 113−127.

Table 3. Dynamic and Static LLS Characterization of PNIPAM-Core Micelles Formed from *Py*-PNIPAM-*b*-POEGMA Diblock Copolymers at $\varphi_{water} = 0.5$

sample codes	$M_{w,LLS}$ (g/mol)	$\langle R_h \rangle$ (nm)	$\langle R_g \rangle$ (nm)	$\langle R_g \rangle / \langle R_h \rangle$	ρ (g/mL)	N_{agg}
Py-PNIPAM$_{75}$-*b*-POEGMA$_{50}$	1.7×10^7	36	28	0.78	0.14	450
Py-PNIPAM$_{75}$-*b*-POEGMA$_{38}$	2.6×10^7	41	33	0.80	0.15	860
Py-PNIPAM$_{75}$-*b*-POEGMA$_{20}$	2.3×10^7	43	34	0.79	0.12	1150
Py-PNIPAM$_{50}$-*b*-POEGMA$_{31}$	5.8×10^7	25	17	0.68	0.15	240
Py-PNIPAM$_{50}$-*b*-POEGMA$_{18}$	9.3×10^6	28	20	0.71	0.22	750

$\approx$ 420 s) should be ascribed to the structural rearrangement and further packing of PNIPAM segments within the micelle core, restricting the mobility of pyrene end groups and decreasing their encountering probability. Winnik[59] reported that I_E/I_M ratios of pyrene-labeled PNIPAM chains also exhibit a decrease during the temperature-induced phase transition. To elucidate the whole micellization process at both short and long time scales, we are currently investigating the micellization kinetics of *Py*-PNIPAM$_{50}$-*b*-POEGMA$_{18}$ via a combination of stopped-flow light scattering and fluorescence.

Figure 9 shows the fluorescence emission spectra of *Py*-PNIPAM$_{50}$-*b*-POEGMA$_{18}$ in a methanol/water mixture at different φ_{water} values, where each spectrum was recorded $\sim$20 min after mixing the copolymer solution in methanol with water. After this time period of storage, we can safely expect that the formed micelles have reached or are quite close to the final equilibrium state on the basis of results presented in Figure 8.

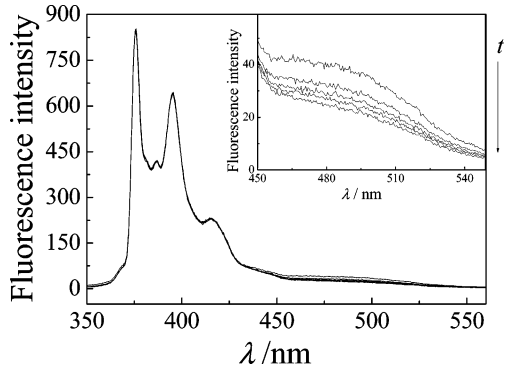

Figure 7. Time dependence of fluorescence spectra of *Py*-PNIPAM$_{50}$-*b*-POEGMA$_{18}$ in methanol/water mixture at $\varphi_{water} = 0.5$. The time intervals between each curve from top to bottom were 5 min. The first spectrum was recorded $\sim$5 s after mixing the copolymer solution in methanol with an equal volume of water. The inset shows the enlarged spectra in the wavelength range of 450−550 nm. The polymer concentration was 1.0 g/L.

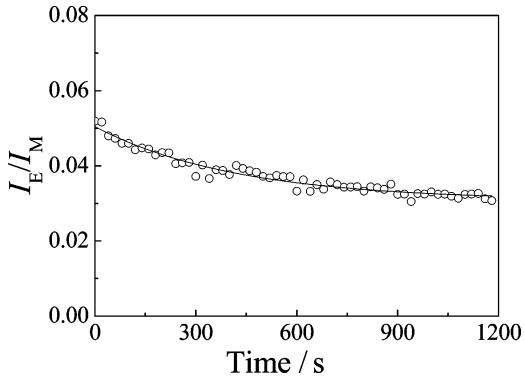

Figure 8. Time dependence of the ratio of excimer-to-monomer fluorescence emission intensity (I_E/I_M) in methanol/water mixture at $\varphi_{water} = 0.5$. The first point ($t = 0$) was measured $\sim$5 s after mixing the copolymer solution in methanol with water. The time intervals between each point were 20 s, and the polymer concentration was 1.0 g/L.

In pure water or methanol, no apparent excimer peak can be discerned, indicating that the copolymer chains are dissolved as unimers. A similar result is obtained for that at $\varphi_{water} = 0.3$. In the final φ_{water} range of 0.5−0.8, we can clearly observe the appearance of the excimer peak.

The variation of I_E/I_M with φ_{water} for *Py*-PNIPAM$_{50}$-*b*-POEGMA$_{18}$ at a fixed copolymer concentration and 25 °C is shown in Figure 10. It can be clearly seen that the I_E/I_M values remain relatively small and almost constant at $\varphi_{water} \leq 0.4$. In the φ_{water} range of 0.5−0.8, I_E/I_M considerably increases, showing a maximum at $\varphi_{water} = 0.67$, indicating the formation of PNIPAM-core micelles induced by cononsolvency and pyrene groups are localized within the micellar core. The φ_{water} range in which I_E/I_M exhibits appreciable deviations from that in pure methanol or water agrees quite well with the previous LLS and ^{1}H NMR results and those reported for the cononsolvency of PNIPAM homopolymers.[27,30,52]

On the basis of LLS results (Tables 2 and 3), the formed PNIPAM-core micelles of *Py*-PNIPAM$_{50}$-*b*-POEGMA$_{18}$ at $\varphi_{water} = 0.5$ possess the highest overall micelle density and molar

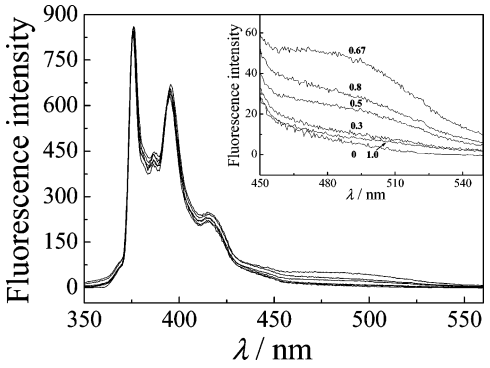

Figure 9. Fluorescence emission spectra of *Py*-PNIPAM$_{50}$-*b*-POEGMA$_{18}$ in methanol/water mixture at different φ_{water} values. The spectra were recorded $\sim$20 min after mixing the copolymer solution in methanol with water. The final copolymer concentration was fixed at 1.0 g/L.

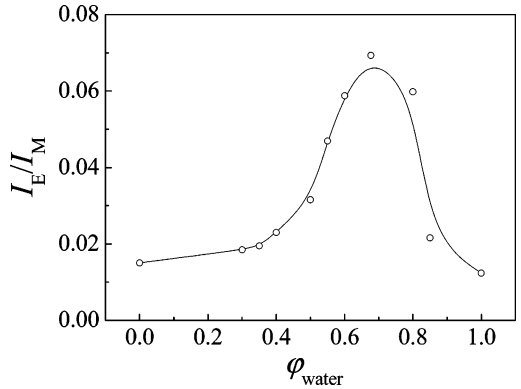

Figure 10. Excimer-to-monomer fluorescence intensity ratios (I_E/I_M) of *Py*-PNIPAM$_{50}$-*b*-POEGMA$_{18}$ in methanol/water mixtures as a function of φ_{water}. The final copolymer concentration was fixed at 1.0 g/L.

mass; however, in the fluorescence results (Figure 10), the I_E/I_M value exhibits a maximum at $\varphi_{water} = 0.67$, instead of at $\varphi_{water} = 0.50$. This discrepancy should be due to the different compactness of micelle cores, tuning the mobility of pyrene end groups and the probability of contact between them.

Conclusion

We investigated the cononsolvency-induced micellization of pyrene end-labeled diblock copolymers, poly(*N*-isopropylacrylamide)-*b*-poly(oligo(ethylene glycol) methyl ether methacrylate), *Py*-PNIPAM-*b*-POEGMA. They molecularly dissolve in pure methanol and water separately, but form well-defined and nearly monodisperse PNIPAM-core micelles in proper mixtures of them (in the φ_{water} range of 0.5−0.8) because of cononsolvency of the PNIPAM block. LLS experiments revealed that the formed micelles possess the highest overall micelle density and molar masses at $\varphi_{water} = 0.5$. The relative block length ratios of *Py*-PNIPAM-*b*-POEGMA also dramatically affect the structural parameters of cononsolvency-induced PNIPAM-core micelles. Upon mixing the diblock copolymer solution in methanol with an equal volume of water ($\varphi_{water} = 0.5$), time-resolved fluorescence measurements reveal that I_E/I_M ratios continuously decrease with time and stabilize out after ∼20 min. The gradual decrease of I_E/I_M with time should be ascribed to the structural rearrangement and further packing of PNIPAM segments within the micelle core. In summary, we successfully demonstrated the first example of cononsolvency-induced unimer−micelle−unimer transition of PNIPAM-containing block copolymers in methanol/water mixtures; moreover, the time scale of the overall micellization process was also explored by time-resolved fluorescence studies.

Acknowledgment. This work was financially supported by an Outstanding Youth Fund (50425310) and research grants (20534020 and 20674079) from the National Natural Scientific Foundation of China (NNSFC), the "Bai Ren" Project and Special Grant (KJCX2-SW-H14) of the Chinese Academy of Sciences, and the Program for Changjiang Scholars and Innovative Research Team in University (PCSIRT).

Supporting Information Available: Specific refractive index increment (d*n*/d*C*) values of *Py*-PNIPAM-*b*-POEGMA diblock copolymers in methanol/water mixtures at different φ_{water} values. This material is available free of charge via the Internet at http://pubs.acs.org.

LA7020148